Journal of Applied Physics ARTICLE scitation.org/journal/jap

Synchrotron based X-ray radiography of convergent shock waves driven by underwater electrical explosion of a cylindrical wire array

Cite as: J. Appl. Phys. **125**, 093301 (2019); doi: 10.1063/1.5089011
Submitted: 16 January 2019 · Accepted: 11 February 2019 ·
Published Online: 1 March 2019

D. Yanuka,[1] S. Theocharous,[1] S. Efimov,[2] S. N. Bland,[1] A. Rososhek,[2] Ya. E. Krasik,[2] M. P. Olbinado,[3] and A. Rack[3]

AFFILIATIONS

[1]Plasma Physics Group, Imperial College London, London SW7 2BW, United Kingdom
[2]Physics Department, Technion—Israel Institute of Technology, Haifa 32000, Israel
[3]European Synchrotron Radiation Facility, CS40220, 38043 Grenoble Cedex 9, France

ABSTRACT

We present X-ray radiography images showing the propagation of shock waves generated by electrical explosion of a cylindrical arrangement of wires in water driven by pulsed power. In previous experiments [S. N. Bland *et al.*, Phys. Plasmas **24**, 082702 (2017)], the merger of shock waves from adjacent wires has produced a highly symmetrical, cylindrical shock wave converging on the axis, where it is expected to produce a high density, strongly coupled plasma ideal for warm dense matter research. However, diagnostic limitations have meant that much of the dynamics of the system has been inferred from the position of the front of the cylindrical shock and timing/spectra of light emitted from the axis. Here, we present a synchrotron-based radiography of such experiments—providing direct quantitative measurements on the formation of the convergent shock wave, the increased density of water on the axis caused by its arrival, and its "bounce" after arrival on the axis. The obtained images are compared with two-dimensional hydrodynamic simulations, which reproduce the observed dynamics with a satisfactory agreement in density values.

I. INTRODUCTION

There has been a growing interest in converging cylindrical shock waves since the early 1940s due to the high densities and energy densities that can be obtained in the vicinity of convergence.[1] Achieving these high energy density states is important in multiple areas of research—for instance, it enables the equation of state (EOS) of highly coupled plasmas to be developed, which underpins the formation of exoplanets and stars whilst directly affecting inertial confinement fusion experiments in laboratory conditions.[2,3] Previous methods of generating converging cylindrical shock waves included using chemical explosives packed around a cylinder, having a dynamic z-pinch strike a cylinder on the axis, and directly or indirectly utilising radiation from high energy laser systems.[4–6] In the last decade, though, much research has been carried out on a relatively new method—using underwater electrical explosions of cylindrical wire arrays to directly generate such shock waves.[7–13] This method had proven to be both easily controllable and highly efficient theoretically enabling small pulsed power drivers to reach multi-Mbar pressures, without requiring the special safety measures necessary in the case of high explosives.

The underwater electrical explosion of wires is characterized by the rapid expansion of the wires as they undergo phase transitions from solid to plasma, which results in the generation of shock waves in the surrounding water. The shock waves from each individual wire in the cylindrical array merge to create a single cylindrical converging shock wave, which generates high energy density conditions in the vicinity of the implosion axis. However, until now, laser shadowgraphy has been the principle diagnostic used to study such experiments—with a powerful continuous-wave laser passing axially through the array which is then recorded via a high-speed framing camera or a streak camera. In practice, shadowgraphy can image only the front of the merged shock wave—image contrast is strongly degraded behind the shock front due to induced turbulence which scatters the laser light. Further limitations in optics and alignment have meant the shock wave cannot be followed all the way to the axis; for instance, in a recent study at Imperial College London, the shock wave dynamics could be followed only from the diameter of

the array (10 mm) until ~100 μm diameter. The stability of the shock wave, which becomes radiative in the vicinity of an implosion, and its velocity then enabled calculations of the pressures closer to the axis, with over 1 Mbar being obtained under a 20 μm diameter.[14] A direct measure of the density on the axis of such experiments would lend much support to previous experiments and the hydrodynamic (HD) calculations used to then infer pressure on/close to the axis, and to the potential use of underwater arrays to drive high pressures in other materials placed on the axis.

In this paper, we present X-ray radiography images of underwater electrical explosions of cylindrical wire arrays, obtained at the European Synchrotron Radiation Facility (ESRF). These images, taken in the phase contrast regime, allow us to see both the merged shock wave produced in the experiments and through the material behind this shock. This allows us to study how the shock waves from the individual wires merge together and the conditions created on the axis at the arrival of the convergent shock. The images also allow us to see the reflection of this shock wave after it reaches the axis as it propagates back to the wire array. Moreover, as well as shock velocities, the water density can be directly measured from the radiographs and compared with a two-dimensional (2D) HD simulation coupled with the EOS of water, which can also provide pressure, temperature, and energy density values.

II. EXPERIMENTAL SETUP

The experiments were carried out at the ID19 beamline at ESRF which is located at 150 m from the undulators. The long distance between source and experiment allows one to use partially coherent X-rays for the imaging experiment. The X-ray beam energy spectrum was polychromatic, ranging from ~20 keV to ~50 keV, with a mean energy of ~30 keV. The photon flux was of 2×10^7 photons/mm^2 before the experimental chamber, with a pulse duration of 100 ps and 176 ns separation between pulses. After the sample, the beam was propagated another 10 m to obtain a propagation-based phase-contrast regime, where diffraction effects increase the contrast of interfaces, i.e., between different material phases where a sudden change of the refractive index occurs. The beam then hits a LYSO:Ce scintillator imaged via a 45° mirror to a Shimadzu HPV-X2 camera with a detector pixel size of 32 μm, which allows capturing an image from every third pulse. A more detailed description of the experimental setup of ID19 is available in Refs. 15 and 16 and the current experimental setup in Ref. 17.

The pulsed power generator consisted of four parallel low-inductance, High-Voltage (HV) Maxwell capacitors of 220 nF each, charged to 32 kV and discharged by a spark gas switch. The cylindrical arrays of 5 mm diameter were constructed using 20 copper wires of 30 mm in length and 63 μm in diameter, chosen to critically damp current and maximise energy transfer rate to the wires. The wires were stretched and soldered between two electrodes screwed in an acrylic tube filled with deionised water. This setup was then placed axially, along the X-ray beam, in an aluminium chamber, which provided the current return path and acted to contain any water spilled/debris produced during an experiment. 10 mm diameter windows covered by thin mylar sheets enabled the X-rays to pass through. The discharge current was measured by a Rogowski coil at the output of the generator, and the voltage was measured using a Tektronix HV voltage divider. A sketch of the experimental setup is presented in Fig. 1.

III. EXPERIMENTAL RESULTS

Prior to driving exploding wires, the total inductance of the driver and load was found by replacing the wires with a thick (non-exploding) copper cylinder of the same length and radius. Treating the resistance of the load then as constant, the period and decay rate of the current pulse in this simple series RLC circuit suggested that the overall inductance was ~450 nH. Comparing the voltage measured across the wire array to $V(t) = \mathrm{I}(t)R(t) + LdI(t)/dt$ allowed the inductance of the array and its connection to be estimated as

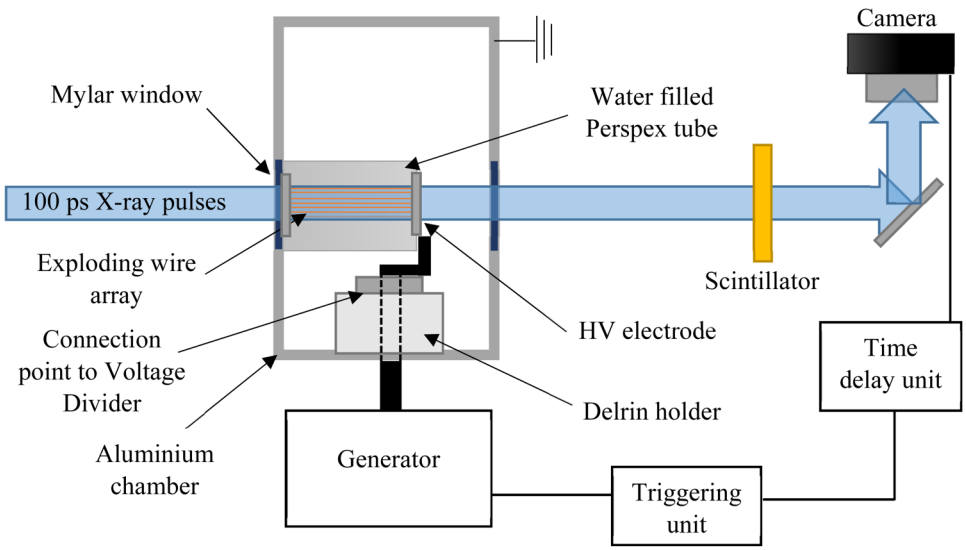

FIG. 1. Experimental setup.

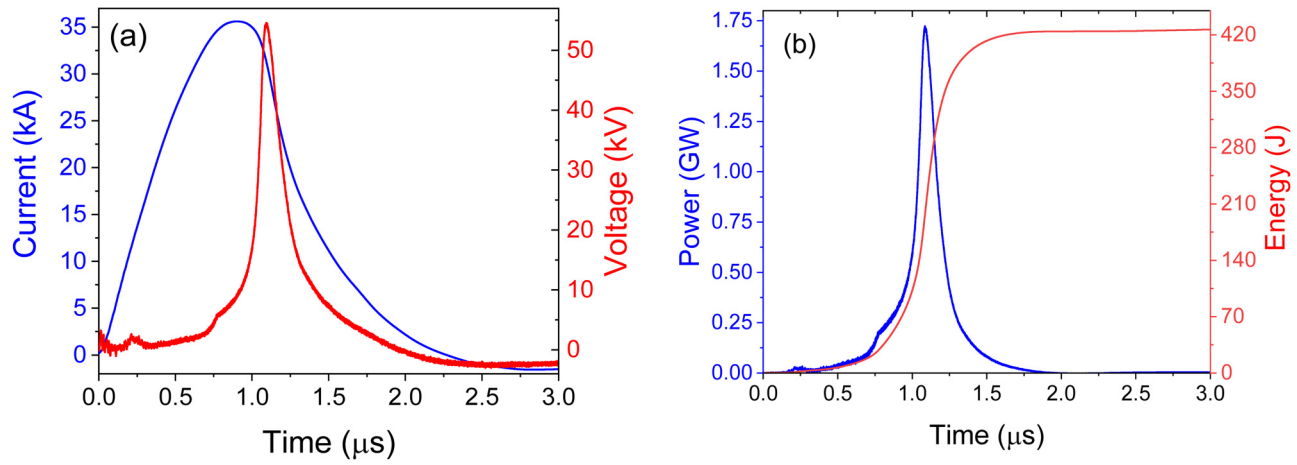

FIG. 2. Current, resistive voltage, power, and energy waveforms.

~50 nH. A theoretical calculation of only the wire array suggests $L \sim 25$ nH, with the rest of the inductance of ~25 nH being due to connections to the driver and the grounded electrode.

The current through and voltage across the array and its connections [corrected for the effects of $LdI(t)/dt$] are shown in Fig. 2. The peak current is ~36 kA at ~0.93 μs and afterwards appears to be slightly underdamped. A simple series circuit with the same inductance and resistance would require a total resistance of ~1.43 Ω for critical damping if the resistance remained constant. In the exploding wire load, however, the resistance varies greatly as the wires are heated and exploded, resulting in the distinct, relatively fast rising voltage pulse and rapid fall in current after peak.

Calculations of the power into the array and total energy deposited into it are also shown in Fig. 2. These suggest that by ~2 μs, as the discharge current becomes negligibly small, a total of ~420 J has been deposited into the wires. This value of deposited energy is slightly lower than the ~450 J initially stored in the capacitors, suggesting some small losses occurring in the spark gap and water surrounding the wire.

The radiography images obtained are presented in Fig. 3. The time stamps are with respect to the beginning of the discharge current [see Fig. 2(a)]. A noticeable expansion of the wires is seen in Fig. 3(c), where the current is slightly after its peak. At this stage, the wire undergoes a transition to the liquid/weakly-ionized gas state where the resistivity rises rapidly followed by the rise in voltage. Then, around the voltage peak of ~55 kV, when the resistance of the wire array reaches ~1.76 Ω, continuing gas ionization leads to a decrease in resistivity and, consequently, to the voltage decreases as well. During the fall of the discharge current, one obtains the main energy deposition into the wires leading to their fast radial expansion and to the launch of a shock wave from each wire.

In the next frame [Fig. 3(d)], a single shock wave is formed as a result of the merged shock waves from the individual wires. Despite the fact that the individual wires do not all expand at the same rate, the self-repairing nature of the shock front in water[13] means that the merged shock wave appears remarkably smooth with no sign of imprint from the wires. The averaged density behind the merged shock was calculated using the X-ray attenuation equation $I = I_0 \exp[-\kappa L\rho]$, where κ is the X-ray mass attenuation coefficient taken from the NIST database for the average ray energy of 30 kV,[18] L is the length of the tube filled with water, ρ is the density of water, and I_0 is the initial ray intensity. This suggests that the water behind the front is ~1.25 g/cm^3 on average and is modulated by the reflecting shocks from the individual wires—with a high of ~1.4 g/cm^3 and a low of ~1.15 g/cm^3.

The average velocity of the shock wave between frames shown in Figs. 3(d) and 3(e) is ~3170 m/s (compared with a speed of sound in water of ~1480 m/s). Considering this velocity to be constant, the shock wave should reach the axis at $t = 1.87$ μs; thus in Fig. 3(e) ($t = 1.96$ μs), the shock wave has just reflected from the axis, i.e., it has "bounced." (In practice, the shock usually accelerates close to the axis; hence, this velocity is, if anything, an underestimate, and so this shock wave must have been reflected by this point in time.) Immediately behind the reflected shock in Fig. 3(e), the average density on/close to the axis is 1.43 g/cm^3. Between Figs. 3(e) and 3(f), the average velocity of the reflected shock is ~3050 m/s. As the reflected shock heads back towards the original array diameter [Fig. 3(g)], the density behind the shock front reduces to ~1.16 g/cm^3.

In Fig. 3(d), one can see a region behind the shock characterized by density non-uniformities arising because of reflecting single shock waves generated by two adjacent wires. In Fig. 3(g), these non-uniformities remain and are squeezed to form straight lines of higher density until they disappear in Fig. 3(h). To decrease these non-uniformities, we are planning to use in future experiments arrays with larger number of wires having smaller diameters.

IV. HYDRODYNAMIC SIMULATION

Two-dimensional HD simulations were run in an attempt to reproduce the features seen in the experiments. These simulations, using a code developed to match previous shadowgraphy data,[19]

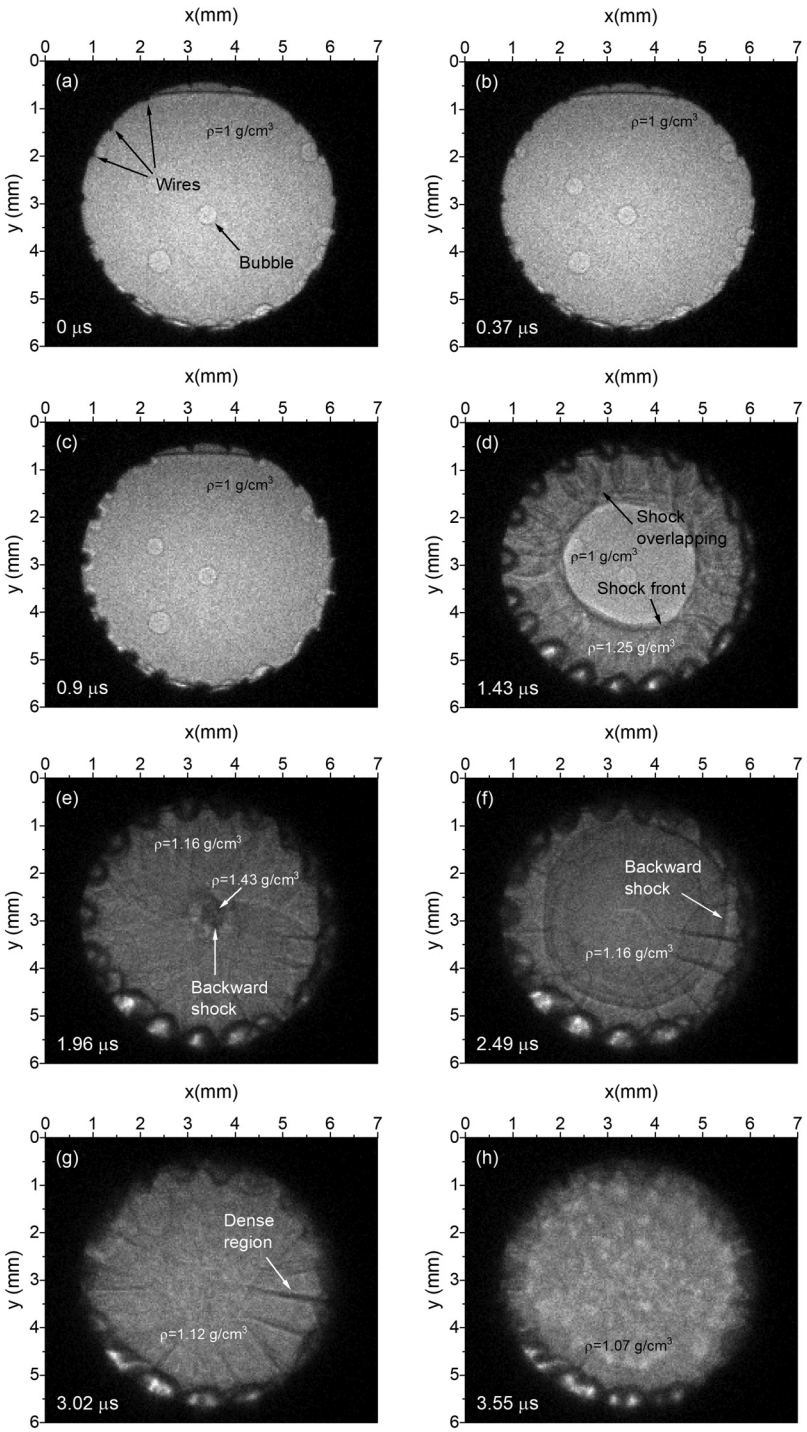

FIG. 3. Radiography images of underwater electrical exploding cylindrical array. {Density values are averaged across [(a)–(c)] water region, (d) non-disturbed water region, and behind the shock front, (e) small circle in the middle and rest of the region, (f) region behind shock propagating back to wires, (g) water region, and (h) water region.}

could now be far better constrained with the density measurements and dynamics of the material behind the shock front. The simulations could also provide information about temperature, energy density, and pressure behind the shock front. The code employed a Lagrangian mesh and considered mass, momentum, and energy conservation equations. These equations were coupled with water and copper EOSs.[20] The input to the simulation was the power calculated from the measured current and resistive voltage in the

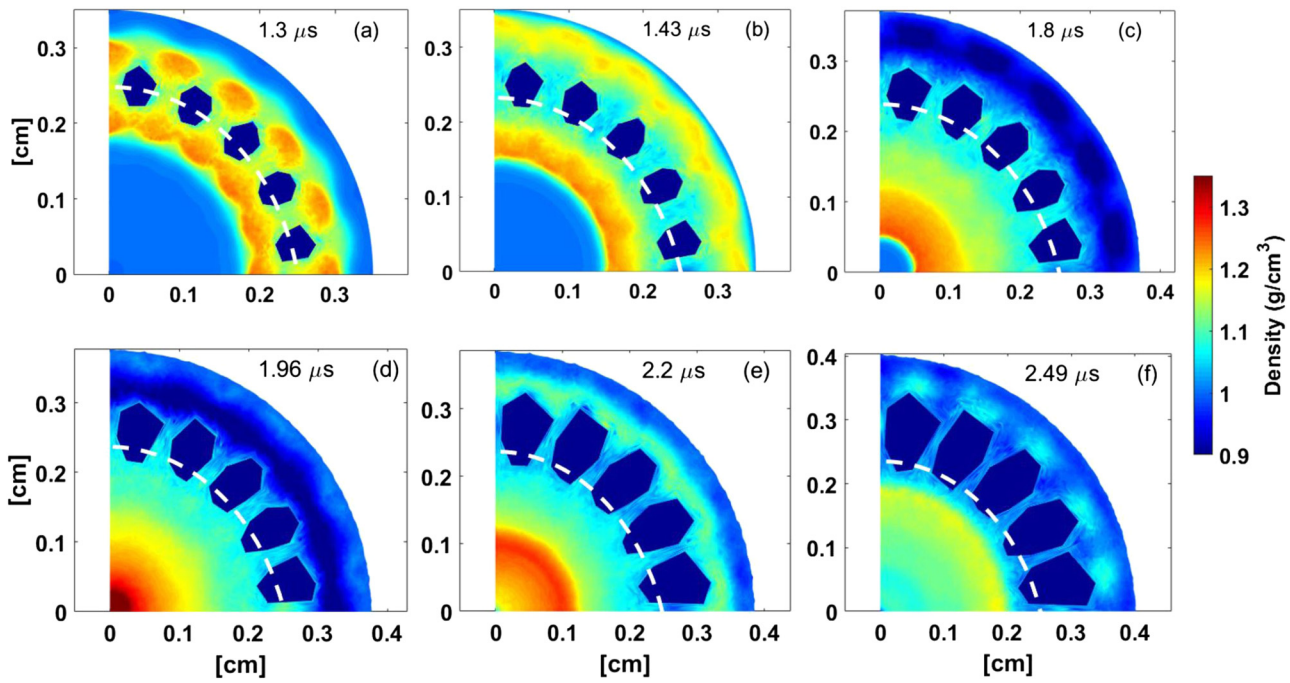

FIG. 4. Hydrodynamic simulation snapshots of density. The white dashed line represents the visible area in the experimental images.

experiment. Similar to previous studies (for example, Ref. 14), only 80% of the deposited power was taken in the hydrodynamic simulation due to possible small losses of current through the surface of the wire and radiation, which do not contribute to the wire's expansion. Generally, in each time step, the power was input to the wires in the simulation and the conservation equations coupled with the EOSs were used to calculate the new pressure, temperature, and density, and the pressure gradient created caused the nodes in the Lagrangian mesh to move. A more detailed description of the algorithm used in the simulation is presented in Ref. 21. Only a quarter of a cylinder was used in order to reduce the running time of the simulation. The boundary condition at $x = 0$ and $y = 0$ is the velocity perpendicular to the boundary $v_{\perp} = 0$.

Six snapshots from the simulation are presented in Fig. 4. Three of these snapshots are at times corresponding to the experimental images in Fig. 3. In Fig. 4(a), one can see the beginning of the process of individual shocks merging to one converging shock wave. The shock keeps converging in Figs. 4(b) and 4(c) and is then reflected back towards the wires in Figs. 4(d)–4(f). The density behind the shock front in Fig. 4(b) is ~1.22 g/cm^3 compared with the experimental 1.25 g/cm^3. The density near the origin in Fig. 4(d) is ~1.34 g/cm^3 compared with the experimental 1.43 g/cm^3, and the density behind the shock going back to the array in Fig. 4(f) is ~1.18 g/cm^3 compared with the experimental 1.16 g/cm^3. Thus, there is a satisfactory agreement in the shock wave's position, as well as the density vales between Figs. 3 and 4 at the respective time delays. The shock reflecting regions pointed out in Fig. 3(d) are also visible in Fig. 4(a) with satisfactory agreement. The simulation was not able to reproduce the dense regions shown in Fig. 3(g). A reason for this can be that the not completely symmetric nature of the explosion caused this dense region to appear. This feature requires additional research.

V. SUMMARY

Synchrotron-based X-ray radiography images of an underwater electrical explosion of a cylindrical wire array were presented. These images allow one to observe the average density of water behind the shock front and after implosion, which was impossible using optical diagnostics. The results were compared with a 2D HD simulation with satisfactory agreement both in the position of the shock wave generated and in the density values in the different regions. This supports the application of the code in estimating the thermodynamic parameter behind shock waves generated by underwater wire explosions with different geometries.

ACKNOWLEDGMENTS

This research was funded by EPSRC, First Light Fusion Ltd., the Institute of Shock Physics, the ESRF User Program, and U.S. Department of Energy under Cooperative Agreement Nos. DE-NA0003764 and DE-SC0018088 and Sandia National Laboratories. The authors would also like to thank Harald Reichert of ESRF, Paul Berkvens and the safety team at ESRF, W. G. Proud and D. Chapman of Imperial College, D. Eakins of Oxford University, F. Zucchini and C. Chauvin of CEA Gramat, and Svetlana Gleizer and Eugene Flyat of the Technion—Israel Institute of Technology for their support in planning these experiments.

REFERENCES

[1]R. W. Perry and A. Kantrowitz, "The production and stability of converging shock waves," J. Appl. Phys. **22**, 878 (1951).

[2]B. A. Remington, "High energy density laboratory astrophysics," Plasma Phys. Control. Fusion **47**, A191 (2005).

[3]M. K. Matzen, M. A. Sweeney, R. G. Adams, J. R. Asay, J. E. Bailey, G. R. Bennet, D. E. Bliss, D. D. Bloomquist, T. A. Brunner, R. B. Campbell, G. A. Chandler, C. A. Coverdale, M. E. Cuneo, J.-P. Davis, C. Deeney, M. P. Desjarlais, G. L. Donovan, C. J. Garasi, T. A. Haill, C. A. Hall, D. L. Hanson, M. J. Hurst, B. Jones, M. D. Knudson, R. J. Leeper, R. W. Lemke, M. G. Mazarakis, D. H. McDaniel, T. A. Mehlhorn, T. J. Nash, C. L. Olson, J. L. Porter, P. K. Rambo, S. E. Rosenthal, G. A. Rochau, L. E. Ruggles, C. L. Ruiz, T. W. L. Stanford, J. F. Seamen, D. B. Sinars, S. A. Slutz, I. C. Smith, K. W. Struve, W. A. Stygar, R. A. Vesey, E. A. Weinbrecht, D. F. Wenger, and E. P. Yu, "Pulsed-power-driven high energy density physics and inertial confinement fusion research," Phys. Plasmas **12**, 055503 (2005).

[4]J. H. Lee and B. H. K. Lee, "Cylindrical imploding shock waves," Phys. Fluids **8**, 2148 (1965).

[5]H. Schoeffmann, H. Schmidt-Kloiber, and E. Reichel, "Time-resolved investigations of laser-induced shock waves in water by use of polyvinylidenefluoride hydrophones," J. Appl. Phys. **63**, 46 (1988).

[6]M. J. Edwards, A. J. MacKinnon, J. Zweiback, K. Shigemori, D. Ryutov, A. M. Rubenchik, K. A. Keilty, E. Liang, B. A. Remington, and T. Ditmire, "Investigation of ultrafast laser-driven radiative blast waves," Phys. Rev. Lett. **87**, 085004 (2001).

[7]Y. E. Krasik, A. Grinenko, A. Sayapin, and V. T. Gurovich, "Generation of sub-Mbar pressure by converging shock waves produced by the underwater electrical explosion of a wire array," Phys. Rev. E **73**, 057301 (2006).

[8]A. Fedotov, A. Grinenko, S. Efimov, and Y. E. Krasik, "Generation of cylindrically symmetric converging shock waves by underwater electrical explosion of wire array," Appl. Phys. Lett. **90**, 201502 (2007).

[9]S. Efimov, A. Fedotov, S. Gleizer, V. T. Gurovich, G. Bazalitski, and Y. E. Krasik, "Characterization of converging shock waves generated by underwater electrical wire array explosion," Phys. Plasmas **15**, 112703 (2008).

[10]G. Bazalitski, V. T. Gurovich, A. Fedotov-Gefen, S. Efimov, and Y. E. Krasik, "Simulation of converging cylindrical GPa-range shock waves generated by wire array underwater electrical explosions," Shock Waves **21**, 321 (2011).

[11]A. Fedotov-Gefen, S. Efimov, L. Gilburd, S. Gleizer, G. Bazalitski, V. T. Gurovich, and Y. E. Krasik, "Extreme water state produced by underwater wire-array electrical explosion," Appl. Phys. Lett. **96**, 221502 (2010).

[12]A. Fedotov-Gefen, S. Efimov, L. Gilburd, G. Bazalitski, V. T. Gurovich, and Y. E. Krasik, "Generation of a 400 GPa pressure in water using converging strong shock waves," Phys. Plasmas **18**, 062701 (2011).

[13]D. Yanuka, A. Rososhek, S. N. Bland, and Y. E. Krasik, "Uniformity of cylindrical imploding underwater shockwaves at very small radii," Appl. Phys. Lett. **111**, 214103 (2017).

[14]S. N. Bland, Y. E. Krasik, D. Yanuka, R. Gardner, J. MacDonald, A. Virozub, S. Efimov, S. Gleizer, and N. Chaturvedi, "Generation of highly symmetric, cylindrically convergent shockwaves in water," Phys. Plasmas **24**, 082702 (2017).

[15]M. P. Olbinado, X. Just, J. Gelet, P. Lhuissier, M. Scheel, P. Vagovic, T. Sato, R. Graceffa, J. Schulz, A. Mancuso, J. Morse, and A. Rack, "MHz frame rate hard X-ray phase-contrast imaging using synchrotron radiation," Opt. Express **25**, 13857 (2017).

[16]M. P. Olbinado, V. Cantelli, O. Mathon, S. Pascarelli, J. Grezner, A. Pelka, M. Roedel, I. Prencipe, A. Garcia, U. Helbig, D. Kraus, U. Schramm, T. Cowan, M. Scheel, P. Pradel, T. De Resseguier, and A. Rack, "Ultra high-speed x-ray imaging of laser-driven shock compression using synchrotron light," J. Phys. D Appl. Phys. **51**, 055601 (2018).

[17]D. Yanuka, A. Rososhek, S. Theocharous, S. N. Bland, Y. E. Krasik, M. P. Olbinado, and A. Rack, "Multi frame synchrotron radiography of pulsed power driven underwater single wire explosions," J. Appl. Phys. **124**, 153301 (2018).

[18]NIST, see https://physics.nist.gov/PhysRefData/XrayMassCoef/ComTab/water.html for X-ray mass attenuation coefficients of water.

[19]D. Yanuka, A. Rososhek, S. Efimov, M. Nitishinskiy, and Y. E. Krasik, "Time-resolved spectroscopy of light emission from plasma generated by a converging strong shock wave in water," Appl. Phys. Lett. **109**, 244101 (2016).

[20]S. P. Lyon and J. D. Johnson, The Los Alamos National Laboratory Equation-of-State Database, LANL Rep. LA UR-92-3407, 1992.

[21]M. Kozlov, V. T. Gurovich, and Y. E. Krasik, "Stability of imploding shocks generated by underwater electrical explosion of cylindrical wire array," Phys. Plasmas **20**, 112701 (2013).